Imaging Science in Dentistry 2024; 54: 313-8
https://doi.org/10.5624/isd.20240029

Effect of a metal artifact reduction algorithm on cone-beam computed tomography scans of titanium and zirconia implants within and outside the field of view

Parisa Soltani[1,2], Amirhossein Moaddabi[3], Mojdeh Mehdizadeh[1], Mohammad Reza Bateni[4], Sepehr Naghdi[4], Mariangela Cernera[2], Farnaz Mirrashidi[5,*], Mohammad Matin Azimipour[4], Gianrico Spagnuolo[2], Alessandra Valletta[2]

[1]*Department of Oral and Maxillofacial Radiology, Dental Implants Research Center, Dental Research Institute, School of Dentistry, Isfahan University of Medical Sciences, Isfahan, Iran*
[2]*Department of Neurosciences, Reproductive and Odontostomatological Sciences, University of Naples Federico II, Naples, Italy*
[3]*Department of Oral and Maxillofacial Surgery, Dental Research Center, Mazandaran University of Medical Sciences, Sari, Iran*
[4]*School of Dentistry, Isfahan University of Medical Sciences, Isfahan, Iran*
[5]*Department of Oral and Maxillofacial Radiology, School of Dentistry, Isfahan University of Medical Sciences, Isfahan, Iran*

ABSTRACT

Purpose: This study aimed to evaluate the impact of a metal artifact reduction (MAR) algorithm on cone-beam computed tomography (CBCT) scans of titanium and zirconia implants, both within and outside the field of view (FOV).

Materials and Methods: In this *in vitro* study, a dry human mandible was positioned in a CBCT scanner with only its left quadrant included in the FOV. Each type of implant (titanium and zirconia) was placed once in the right second premolar extraction socket and once in the left second premolar extraction socket of the mandible. CBCT scans were acquired with and without MAR. Three regions of interest (ROIs) were defined in relation to a resin block, and the contrast-to-noise ratio (CNR) was calculated for each ROI. Data were analyzed using 2-way analysis of variance with an alpha level of 0.05.

Results: Application of a MAR algorithm significantly increased the CNR within and outside the FOV for both implant types ($P<0.05$). Relative to titanium implants, zirconia implants were associated with significantly lower CNRs in both positions ($P<0.05$) and generated more artifacts. Implant placement outside the FOV was associated with slightly lower image quality than positioning within the FOV, although this finding was not significant ($P>0.05$).

Conclusion: The results suggest that application of a MAR algorithm in CBCT significantly impacts artifact generation. Titanium implants exhibited significantly lower metal artifact generation compared to zirconia implants. Positioning either implant type outside the FOV, as opposed to inside it, slightly increased artifact generation; however, this was not statistically significant. ***(Imaging Sci Dent 2024; 54: 313-8)***

KEY WORDS: Cone-Beam Computed Tomography; Artifacts; Dental Implants; Mandible

Introduction

Contemporary dentistry strives to restore masticatory function while ensuring acceptable dental esthetics. In pursuit of this goal, dental implants represent an ideal solution for replacing teeth lost to periodontal disease or trauma.[1]

Titanium and its alloys are widely utilized in the production of dental implants. Nevertheless, concerns over immunological reactions and esthetic issues associated with titanium implants have prompted researchers to explore other materials. Zirconia implants have emerged as

This research was financially supported by the School of Dentistry, Isfahan University of Medical Sciences, Isfahan, Iran. (3402294)
Received February 18, 2024; Revised May 11, 2024; Accepted May 28, 2024
Published online August 25, 2024
*Correspondence to : Prof. Farnaz Mirrashidi
Department of Oral and Maxillofacial Radiology, School of Dentistry, Isfahan University of Medical Sciences, Hezar-Jarib Ave, Isfahan 8174673461, Iran
Tel) 98-313-792-5508, E-mail) Fs.mirrashidi@gmail.com

Copyright ⓒ 2024 by Korean Academy of Oral and Maxillofacial Radiology
This is an Open Access article distributed under the terms of the Creative Commons Attribution Non-Commercial License (http://creativecommons.org/licenses/by-nc/3.0) which permits unrestricted non-commercial use, distribution, and reproduction in any medium, provided the original work is properly cited.
Imaging Science in Dentistry · pISSN 2233-7822 eISSN 2233-7830

an alternative to titanium implants. Zirconia is considered suitable for implants because of its tooth-like color, optimal mechanical properties, favorable biocompatibility, and low plaque adhesion.[2]

In clinical settings, cone-beam computed tomography (CBCT) is frequently requested for preoperative assessment in dental implant placement, based on the patient's medical and dental history, clinical examination, and initial periapical or panoramic radiographs. However, a major drawback of CBCT is the presence of artifacts. Materials with high density and high atomic number can generate metal artifacts on CBCT images.[3] These artifacts compromise the quality of the images and can distort the depiction of anatomical structures and defects in the vicinity of metal objects.[4] To mitigate the impact of CBCT artifacts, complex algorithms have been developed. Among these, the metal artifact reduction (MAR) algorithm is widely implemented for diagnostic purposes when metal objects are present within the field of view (FOV).[5]

A previous study indicated that zirconia implants produce more metal artifacts than titanium implants.[6] In separate research, Khosravifard et al.[7] found that decreasing the size of the FOV significantly reduced streak artifacts. Nascimento et al.[8] reported that neither the tube current (mA) nor application of the MAR algorithm significantly affected the detection of peri-implant dehiscence. Another study notably observed that dental implants generated more pronounced artifacts when positioned within the FOV than when located outside of it;[9] however, 2 different FOVs were employed. Thus, it is imperative to evaluate artifact generation by implants both within and outside the FOV while maintaining a consistent FOV size. Additionally, comparing the efficacy of different software programs for MAR could reveal more effective algorithms. The present study aimed to assess the impact of a MAR algorithm on CBCT scans of titanium and zirconia implants, both within and outside the FOV.

Materials and Methods

This *in vitro* experimental study was conducted using a dry human mandible along with 1 titanium and 1 zirconia dental implant. The study protocol received approval from the Research Ethics Committee at Isfahan University of Medical Sciences (IR.MUI.RESEARCH.REC.1402.188), with an approval date of August 19, 2023.

Sample size

The minimum sample size was calculated to be 80 CBCT scans, based on an alpha of 5%, a study power of 80%, and an effect size of 0.4. The aim was to compare 5 different scenarios: no implant, a zirconia implant within the FOV, a zirconia implant outside the FOV, a titanium implant within the FOV, and a titanium implant outside the FOV. The 1-way analysis of variance (ANOVA) function of G*Power (version 3.1; Heinrich-Heine University, Düsseldorf, Germany) was used for this purpose, with a significance level of 0.05.

Model preparation

In this study, a titanium dental implant with a 4-mm diameter and 12-mm height (Bionic; Nik Kasht Asia, Tehran, Iran) and a zirconia implant of the same dimensions (White Sky; Bredent Medical, Senden, Germany) were used. The titanium implant was crafted from type V titanium alloy, consisting of 60 wt% aluminum and 40 wt% vanadium. The zirconia implant was composed of zirconium dioxide along with a small amount of yttrium.

A dry human mandible, obtained from the archives of the Oral and Maxillofacial Radiology Department, was wrapped in a single layer of baseplate wax (Polywax; Bilkilm, Izmir, Turkey) with a thickness of 6 mm to simulate the soft tissue. An epoxy resin block, measuring 9 mm × 4 mm × 4 mm, was affixed to the buccal cortical plate of the mandible to serve as a reference point. The block was positioned so that its transverse midpoint aligned with the anteroposterior midline and was perpendicular to it, while its vertical midpoint corresponded to the vertical center of the dental implant (Fig. 1).

CBCT imaging

All images were acquired using a single CBCT scanner (Galileos; Sirona Dental Systems, Bensheim, Germany) with the following exposure settings: an FOV of 8 cm × 15 cm, a tube current of 10 mA, a tube potential of 85 kVp, and a voxel size of 0.280 mm. The mandible was positioned in the CBCT scanner so that its left side fell within the FOV, while its right side was outside the FOV. Each type of implant (titanium/zirconia) was inserted once into the right second premolar extraction socket and once into the left second premolar extraction socket of the mandible, followed by scanning. Consequently, when the implant was placed in the left quadrant of the mandible, it was within the FOV, whereas placement in the right quadrant meant it was outside the FOV. CBCT scans were obtained 8 times in the control position (without an implant) and 8 times for each experimental condition (with zirconia and titanium implants, within and outside the FOV).

The MAR algorithm of Sidexis 4 software (Sirona Dental Systems) was utilized for image interpretation. Each image was examined both with and without MAR application. In total, 80 CBCT scans were evaluated.

Analysis of CBCT images

The Digital Imaging and Communications in Medicine file containing the CBCT images was transferred to ImageJ (National Institutes of Health, Bethesda, MD, USA).[10] Three regions of interest (ROIs) measuring 12 mm × 3 mm were selected in relation to the resin block.[9] To define these areas, a horizontal line was drawn tangent to the mesial surface of the second premolar root, and a vertical line was drawn from the center of the resin block by the observer. The central ROI was positioned at the vertical midpoint of the resin block, with the other 2 ROIs placed 3 mm to the right and left of the central ROI (Fig. 2). An additional ROI was also chosen at the midpoint of the resin block to serve as a control. Subsequently, the contrast-to-noise ratio (CNR) was calculated using the mean and standard deviation of the gray values of the pixels within each ROI, applying the following formula:

$$CNR = \frac{|Mean_{implant} - Mean_{control}|}{\sqrt{SD^2_{implant} + SD^2_{control}}}$$

For each image, the mean CNR of the 3 ROIs was calculated and recorded as the total CNR.

Fig. 1. Model prepared for cone-beam computed tomography scans.

Statistical analysis

Data were analyzed using IBM SPSS Statistics 24 (IBM Corp., Armonk, NY, USA). The normal distribution of the data was confirmed using the Kolmogorov-Smirnov test ($P > 0.05$). Accordingly, the data are presented as the mean ± standard deviation. A 2-way ANOVA model was used to evaluate the effects of implant type, implant position, and MAR application on the CNR. *P*-values less than 0.05 were considered to indicate statistical significance.

Results

Table 1 summarizes the CNR findings based on MAR

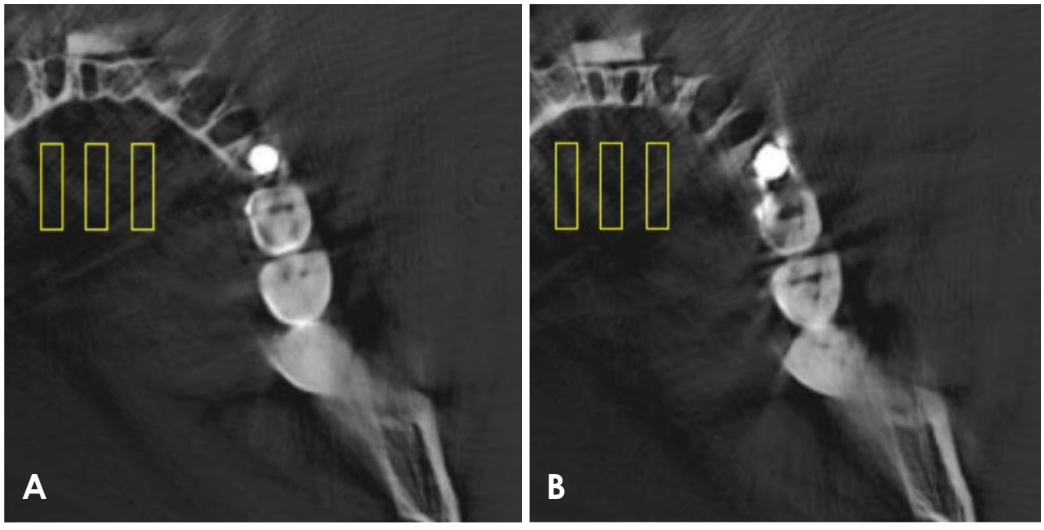

Fig. 2. Selected regions of interest in ImageJ software with titanium (A) and zirconia (B) implants, positioned within the field of view on axial cone-beam computed tomography images.

Table 1. Effect of position and metal artifact reduction (MAR) on contrast-to-noise ratio for titanium and zirconia implants

Type	Position	MAR	Contrast-to-noise ratio
Titanium	Within	On	14.73 ± 0.07
		Off*	14.09 ± 0.08
	Outside	On	14.36 ± 0.11
		Off*	14.01 ± 0.5
Zirconia	Within	On	13.32 ± 0.62
		Off*	12.41 ± 0.52
	Outside	On	13.32 ± 0.87
		Off*	12.29 ± 0.42

*$P < 0.05$ compared to MAR activated (on) regardless of position

Table 2. Effect of metal artifact reduction (MAR) and implant type on contrast-to-noise ratio within and outside the field of view

Position	MAR	Type	Contrast-to-noise ratio
Within	On	Titanium	14.73 ± 0.07
		Zirconia**	13.32 ± 0.62
	Off*	Titanium	14.09 ± 0.08
		Zirconia**	12.41 ± 0.52
Outside	On	Titanium	14.36 ± 0.11
		Zirconia**	13.32 ± 0.87
	Off*	Titanium	14.01 ± 0.5
		Zirconia**	12.29 ± 0.42

*$P < 0.05$ compared to MAR activated (on) regardless of implant type, **$P < 0.05$ compared to titanium implant regardless of MAR application

application at each position for the 2 implant types. The model revealed no significant interaction between position and MAR for either type of implant. Furthermore, the effect of position on CNR was not significant for either titanium or zirconia implants. However, MAR significantly impacted CNR for both implant types. Specifically, the mean CNR with MAR applied was higher than with MAR not applied for both titanium and zirconia implants.

Table 2 presents the CNR findings based on implant type for each MAR status at the 2 implant positions. The model revealed no significant interaction between MAR and implant type at either position (within and outside the FOV). However, the effects of MAR and implant type on CNR were significant for both positions. Specifically, the mean CNR with MAR applied was higher than with MAR not applied, both within and outside the FOV. Additionally, the mean CNR for titanium implants was greater than that for zirconia implants at both positions.

Table 3. Effect of implant type and position on contrast-to-noise ratio with metal artifact reduction (MAR) either applied or not applied

MAR	Type	Position	Contrast-to-noise ratio
On	Titanium	Within	14.73 ± 0.07
		Outside	14.36 ± 0.11
	Zirconia*	Within	13.32 ± 0.62
		Outside	13.32 ± 0.87
Off	Titanium	Within	14.09 ± 0.08
		Outside	14.01 ± 0.5
	Zirconia*	Within	12.41 ± 0.52
		Outside	12.29 ± 0.42

*$P < 0.05$ compared to titanium implant regardless of position

Table 3 summarizes the CNR findings based on implant position for each type, with MAR either applied or not applied. The model revealed no significant interaction between type and position for either MAR setting. Furthermore, the effect of position on CNR was not significant in either MAR mode. However, the effect of implant type on CNR was significant in both modes. Consequently, the mean CNR for titanium implants was higher than that of zirconia implants, regardless of MAR application.

Discussion

The present study evaluated the impact of MAR algorithm application on CBCT scans of titanium and zirconia implants, placed within and outside the FOV. The findings indicated that using the MAR algorithm significantly influenced the CNR when a titanium or zirconia implant was present, irrespective of its position relative to the FOV. Zirconia implants exhibited a lower CNR and subsequently generated more pronounced artifacts compared to titanium implants. The placement of titanium or zirconia implants outside the FOV resulted in marginally lower image quality than placement within the FOV, although this finding was not statistically significant. A higher CNR within a region denotes superior image quality with reduced noise, whereas a lower CNR indicates increased noise and, consequently, diminished image quality.

Vasconcelos et al.[6] reported that zirconia implants produce more metal artifacts than titanium implants. They also noted that adjusting exposure settings, such as increasing the tube voltage (kVp) and applying a MAR algorithm, can

improve image quality with respect to metal artifact generation. The present results corroborate their findings of increased metal artifact generation with zirconia compared to titanium implants; however, in the current study, the impact of exposure parameters on artifact generation was not assessed. Demirturk Kocasarac et al.[9] found that artifacts were less pronounced when dental implants were located within the FOV rather than outside it. In the present study, the CNR was marginally higher, although not significantly so, when dental implants were positioned outside the FOV. Notably, Demirturk Kocasarac et al.[9] utilized a smaller FOV for implants outside the FOV than for those within the FOV. Previous research has established that using a smaller FOV can reduce artifact generation.[7] Consequently, in the present study, a consistent FOV was used for implants both within and outside the FOV by offsetting the dry mandible and placing the dental implants in its right and left quadrants.[11]

Fontenele et al.[12] conducted CBCT scans on a dry human mandible with and without a zirconia implant in 3 modes: without MAR, with MAR applied before exposure, and with MAR applied after exposure. The authors quantified artifact generation by calculating the standard deviation and CNR at 6 ROIs with varying distances and angles from the dental implant. Their findings indicated that the application of MAR in either mode reduced CBCT artifacts, particularly in areas where artifacts more heavily impacted image quality. The efficacy of MAR reported in their study aligns with the present results. However, while Fontenele et al.[12] utilized the OP300 Maxio scanner for their research, the present study employed the Galileos scanner.

In a separate study by Fontenele et al.,[13] the impact of MAR on the detection of peri-implant defects was examined. The researchers determined that the use of MAR does not influence the identification of dehiscences near zirconia and titanium-zirconia implants. Additionally, they reported higher sensitivity and lower specificity for detecting these dehiscences when zirconia implants, as opposed to titanium-zirconia implants, were present. The Picasso Trio scanner was utilized by Fontenele et al. for that research.[13]

Notably, the present study was limited by its *in vitro* design. Further research should involve CBCT scans of actual patients. Additionally, this study did not evaluate artifact generation occurring after the activation of the MAR algorithm prior to exposure; this aspect warrants attention in future studies. Furthermore, the effects of various MAR software programs on CBCT scans, obtained with different CBCT scanners and exposure parameters, should be evaluated.

In conclusion, the findings indicate that the application of a MAR algorithm significantly impacted artifact generation on CBCT images of titanium and zirconia implants. The titanium implant was associated with significantly lower generation of metal artifacts than the zirconia implant. Placing titanium/zirconia implants outside the FOV, as opposed to inside the field, marginally increased the magnitude of artifact generation; however, this increase was not statistically significant.

Conflicts of Interest: None

References

1. Thoma DS, Gil A, Hämmerle CH, Jung RE. Management and prevention of soft tissue complications in implant dentistry. Periodontol 2000 2022; 88: 116-29.
2. Özkurt Z, Kazazoğlu E. Zirconia dental implants: a literature review. J Oral Implantol 2011; 37: 367-76.
3. Queiroz PM, Santaella GM, Groppo FC, Freitas DQ. Metal artifact production and reduction in CBCT with different numbers of basis images. Imaging Sci Dent 2018; 48: 41-4.
4. Chagas MM, Kobayashi-Velasco S, Gimenez T, Cavalcanti MG. Diagnostic accuracy of imaging examinations for peri-implant bone defects around titanium and zirconium dioxide implants: a systematic review and meta-analysis. Imaging Sci Dent 2021; 51: 363-72.
5. Candemil AP, Salmon B, Freitas DQ, Ambrosano GM, Haiter-Neto F, Oliveira ML. Are metal artefact reduction algorithms effective to correct cone beam CT artefacts arising from the exomass? Dentomaxillofac Radiol 2019; 48: 20180290.
6. Vasconcelos TV, Leandro Nascimento EH, Bechara BB, Freitas DQ, Noujeim M. Influence of cone beam computed tomography settings on implant artifact production: zirconia and titanium. Int J Oral Maxillofac Implants 2019; 34: 1114-20.
7. Khosravifard A, Saberi BV, Khosravifard N, Motallebi S, Kajan ZD, Ghaffari ME. Application of an auto-edge counting method for quantification of metal artifacts in CBCT images: a multivariate analysis of object position, field of view size, tube voltage, and metal artifact reduction algorithm. Oral Surg Oral Med Oral Pathol Oral Radiol 2021; 132: 735-43.
8. Nascimento EH, Imbelloni-Vasconcelos AC, Fontenele RC, Gaêta-Araujo H, Moraes Ramos-Perez FM, Freitas DQ. Influence of the milliamperage and artifact reduction tool on the cbct-based diagnosis of buccal and lingual peri-implant dehiscences: comparison between two types of implants. Int J Oral Maxillofac Implants 2022; 37: 1202-9.
9. Demirturk Kocasarac H, Koenig LJ, Ustaoglu G, Oliveira ML, Freitas DQ. CBCT image artefacts generated by implants located inside the field of view or in the exomass. Dentomaxillofac Radiol 2022; 51: 20210092.
10. Rueden CT, Schindelin J, Hiner MC, DeZonia BE, Walter AE, Arena ET, et al. ImageJ2: ImageJ for the next generation of scientific image data. BMC Bioinformatics 2017; 18: 529.
11. Farias-Gomes A, Fontenele RC, Rosado LP, Neves FS, Freitas

DQ. The metal post material influences the performance of artefact reduction algorithms in CBCT images. Braz Dent J 2022; 33: 31-40.

12. Fontenele RC, Nascimento EH, Santaella GM, Freitas DQ. Does the metal artifact reduction algorithm activation mode influence the magnitude of artifacts in CBCT images? Imaging Sci Dent 2020; 50: 23-30.
13. Fontenele RC, Nascimento EH, Imbelloni-Vasconcelos AC, Martins LA, Pontual AD, Ramos-Perez FM, Freitas DQ. Influence of kilovoltage-peak and the metal artifact reduction tool in cone-beam computed tomography on the detection of bone defects around titanium-zirconia and zirconia implants. Imaging Sci Dent 2022; 52: 267-73.